NIH Public Access
Author Manuscript
Cancer Discov. Author manuscript; available in PMC 2015 August 01.

Published in final edited form as:
Cancer Discov. 2015 February ; 5(2): 143–153. doi:10.1158/2159-8290.CD-14-0856.

PI3′-Kinase Inhibition Forestalls the Onset of MEK1/2 Inhibitor Resistance in *BRAF*-Mutated Melanoma

Marian M. Deuker[1], **Victoria Marsh Durban**[1,3], **Wayne A. Phillips**[2], and **Martin McMahon**[1,4]

[1]Helen Diller Family Comprehensive Cancer Center & Department of Cell and Molecular Pharmacology, University of California, San Francisco, CA, USA

[2]Peter MacCallum Cancer Centre, Melbourne, Victoria, Australia

Abstract

Phosphatidylinositide 3′ (PI3′)-lipid signaling cooperates with oncogenic $BRAF^{V600E}$ to promote melanomagenesis. Sustained PI3′-lipid production commonly occurs via silencing of the PI3′-lipid phosphatase PTEN or, less commonly, through mutational activation of *PIK3CA*, encoding the 110kDa catalytic subunit of PI3′-kinase-α (PI3Kα). To define the PI3K catalytic isoform dependency of *BRAF*-mutated melanoma, we utilized pharmacologic, isoform-selective PI3K inhibitors in conjunction with melanoma-derived cell lines and genetically engineered mouse (GEM) models. While $BRAF^{V600E}$/$PIK3CA^{H1047R}$ melanomas were sensitive to the anti-proliferative effects of selective PI3Kα blockade, inhibition of $BRAF^{V600E}$/$PTEN^{Null}$ melanoma proliferation required combined blockade of PI3Kα, δ and γ, and was insensitive to PI3Kβ blockade. In GEM models, isoform-selective PI3K inhibition elicited cytostatic effects, but significantly potentiated melanoma regression in response to $BRAF^{V600E}$ pathway-targeted inhibition. Interestingly, PI3K inhibition forestalled the onset of MEK inhibitor resistance in two independent GEM models of $BRAF^{V600E}$-driven melanoma. These results suggest that combination therapy with PI3K inhibitors may be a useful strategy to extend the duration of clinical response of *BRAF*-mutated melanoma patients to $BRAF^{V600E}$ pathway-targeted therapies. (Words: 165)

Keywords

Melanoma; $BRAF^{V600E}$; PI3′-kinase; Genetically engineered mouse model; Pre-clinical therapeutics

[4]Corresponding Author: Martin McMahon Ph.D., University of California San Francisco, Helen Diller Family Comprehensive Cancer Center, 1450 Third Street, San Francisco, CA 94158, USA, mcmahon@cc.ucsf.edu.
[3]Current Address: European Cancer Stem Cell Research Institute, Cardiff University, School of Biosciences, Cardiff, UK

AUTHOR CONTRIBUTIONS

MMD, VMD and MM designed the study. MMD collected and analyzed data. WAP provided mouse strains. MMD and MM drafted the manuscript. MM supervised the research and assisted in data analysis and interpretation. All authors critically appraised the manuscript and approved its submission.

Conflict of interest statement: Dr. McMahon has received grant support from Novartis Inc.

NIH-PA Author Manuscript
NIH-PA Author Manuscript
NIH-PA Author Manuscript

NIH-PA Author Manuscript
NIH-PA Author Manuscript
NIH-PA Author Manuscript

INTRODUCTION

Over the past fifteen years, key genetic lesions that initiate melanomagenesis, promote disease progression and remain necessary for melanoma maintenance have been identified (1, 2). Approximately 50% of melanomas express mutationally activated $BRAF^{V600E}$, leading to constitutive activation of the $BRAF^{V600E}$→MEK1/2→ERK1/2 mitogen-activated protein (MAP) kinase pathway (3). The importance of this pathway in melanoma maintenance is highlighted by the ability of $BRAF^{V600E}$ pathway-targeted inhibitors to elicit dramatic tumor regression in *BRAF*-mutated, advanced melanoma patients (4–6). Although the response rate of such patients is high, the depth and durability of response is limited by the onset of drug resistant disease that is largely refractory to additional $BRAF^{V600E}$ pathway-targeted therapy (7, 8). Therefore, it is critical to identify signaling pathways that contribute to *de novo* or acquired drug resistance, and to determine if pharmacological blockade of these pathways can increase the response rate or the durability of response to $BRAF^{V600E}$ pathway-targeted therapies. Although multiple mechanisms of acquired drug resistance have been documented, it remains unclear the extent to which parallel inhibition of signaling pathways will enhance melanoma patient responses (9, 10).

Using genetically engineered mouse (GEM) models, we previously demonstrated that either PTEN silencing or mutationally activated $PIK3CA^{H1047R}$ cooperates with $BRAF^{V600E}$ to elicit metastatic melanoma. However, $BRAF^{V600E}$/$PIK3CA^{H1047R}$ melanomas grew more slowly than similarly elicited $BRAF^{V600E}$/$PTEN^{Null}$ melanomas (11). In addition, although a pan-class I PI3K inhibitor (BKM120) significantly potentiated the ability of a $BRAF^{V600E}$ inhibitor (LGX818) to induce regression of autochthonous $BRAF^{V600E}$/$PTEN^{Null}$ melanomas, BKM120 was largely ineffective as a single agent (11). Given the frequency of alterations in PI3′-lipid signaling in *BRAF*-mutated melanoma (12–15), we wished to explore the role of PI3K signaling in melanoma progression and maintenance, as well as the therapeutic implications of targeting this pathway using isoform-selective inhibitors. Our studies reveal that the difference in growth rate between $BRAF^{V600E}$/$PIK3CA^{H1047R}$ and $BRAF^{V600E}$/$PTEN^{Null}$ melanomas is likely due to the strength of PI3K pathway activation. However, potent blockade of PI3K signaling in either $BRAF^{V600E}$/$PIK3CA^{H1047R}$ or $BRAF^{V600E}$/$PTEN^{Null}$ melanomas elicited largely cytostatic effects. Finally, and most interestingly, combined blockade of $BRAF^{V600E}$ and PI3K signaling significantly enhanced the depth and durability of the response of $BRAF^{V600E}$/$PIK3CA^{H1047R}$ or $BRAF^{V600E}$/$PTEN^{Null}$ melanoma to the MEK1/2 inhibitor GDC-0973. These data provide a scientific rationale for the clinical deployment of such regimens for *BRAF*-mutated melanoma patients in which the PI3K pathway is activated either by *PTEN* silencing or *PIK3CA* mutation.

RESULTS

PTEN is reported to have both phosphatase-dependent and -independent tumor suppressor activities (16–18). To address whether differences in growth rate between $BRAF^{V600E}$/$PIK3CA^{H1047R}$ and $BRAF^{V600E}$/$PTEN^{Null}$ melanoma reflect a role for phosphatase-independent tumor suppressor activities of PTEN, we compared the growth rate of *BRAF*-mutated melanomas in *Tyr::CreER; BRaf*^{CA} mice that were homozygous for the *Pten*$^{lox4-5}$ allele or either heterozygous or homozygous for the conditional Cre-activated

NIH-PA Author Manuscript NIH-PA Author Manuscript NIH-PA Author Manuscript

Pik3ca$^{lat\text{-}1047R}$ (*Pik3ca*^{lat} hereafter) allele (Fig. 1A). As shown previously (11), BRAF^{V600E}/PTEN^{Null} melanomas grew more rapidly than BRAF^{V600E}/PIK3CA^{H1047R} melanomas arising in heterozygous *Pik3ca*$^{lat/+}$ mice (Fig. 1A). However, BRAF^{V600E}/PIK3CA^{H1047R} melanomas arising in homozygous *Pik3ca*$^{lat/lat}$ mice grew significantly more rapidly than BRAF^{V600E}/PTEN^{Null} melanomas, suggesting that differences in melanoma growth rate between BRAF^{V600E}/PIK3CA^{H1047R} and BRAF^{V600E}/PTEN^{Null} melanoma are likely due to the magnitude of PI3K pathway activation. In addition, cell lines derived from BRAF^{V600E}/PTEN^{Null}/CDKN2A^{Null} (B10C) or BRAF^{V600E}/PIK3CA$^{H1047R/H1047R}$/CDKN2A^{Null} (BP_2C) melanomas grew more rapidly *in vitro* than did a cell line derived from a BRAF^{V600E}/PIK3CA$^{H1047R/+}$/CDKN2A^{Null} (BPC) melanoma (unpublished observation).

To determine the PI3K isoform dependence of *BRAF*-mutated melanoma, we treated BPC and B10C melanoma cell lines with pharmacological inhibitors of PI3K (Supp. Table 1). BPC melanoma cells treated with BYL719, a selective inhibitor of PI3′-kinase-α (PI3Kα) (19), displayed a robust reduction in cell proliferation over a 72-hour time period and colony forming ability over a ten-day period (Figs. 1B & 1C). By contrast, BYL719 treatment of B10C melanoma cells elicited only a modest reduction in short-term cell proliferation and had no effect on long-term colony formation (Figs. 1B & 1C). Indeed, there was a greater than 10-fold difference between the concentration of BYL719 required for 50% inhibition of proliferation (GI_{50}) of BPC versus B10C cells (Fig. 1D). In addition, the BP_2C melanoma cell line derived from homozygous *Pik3ca*$^{lat/lat}$ mice displayed similar sensitivity to BYL719 as did the BPC cells (Figs. S1A & S1B). Thus, BRAF^{V600E}/PIK3CA^{H1047R} melanoma cells display the predicted genotype-drug response phenotype relationship. By contrast, BRAF^{V600E}/PTEN^{Null} melanoma cells appear not to depend solely on PI3Kα for their proliferation.

To examine the effects of PI3Kα blockade on signal pathway activity, extracts of BPC or B10C melanoma cells treated with BYL719 (5μM) were subjected to immunoblot analysis (Fig. 1E). In BPC cells, BYL719 elicited a complete and sustained inhibition of pAKT (pS473) over 72 hours. We also noted diminished phosphorylation of downstream pathway components of PI3K→AKT signaling including PRAS40 and 4E-BP1 (Fig. 1E). By contrast, BYL719-treated B10C cells displayed only a partial and transient inhibition of pAKT with almost no effect on pPRAS40 or p4E-BP1.

Since BRAF^{V600E} and PI3K signal cooperatively through mTORC to regulate melanoma cell proliferation (20), we investigated whether PI3Kα inhibition would enhance the effects of BRAF^{V600E} inhibition in BPC or B10C melanoma cells. While single agent BRAF^{V600E} (LGX818) (21) or PI3Kα (BYL719) inhibition potently suppressed BPC melanoma cell proliferation, combined treatment elicited a significantly greater inhibition of cell proliferation at 24, 48, and 72 hours (Fig. 1F). Further, while inhibition of PI3Kα suppressed pPRAS40, pRPS6 and p4EB-P1 in BPC melanoma cells, combined inhibition of both BRAF^{V600E} and PIK3CA^{H1047R} signaling elicited a more robust inhibition of these phosphorylation events (Fig. 1G). Similar observations were made in the independently derived BP_2C melanoma cell line (Fig. S1C). By contrast, while BRAF^{V600E} inhibition (LGX818) potently suppressed B10C cell proliferation, addition of BYL719 did not

NIH-PA Author Manuscript

NIH-PA Author Manuscript

NIH-PA Author Manuscript

significantly enhance the anti-proliferative effects of $BRAF^{V600E}$ inhibition at any time point (Fig. 1F). In B10C cells, LGX818 inhibited pERK but had little effect on pRPS6 or p4E-BP1 (Fig. 1G). Although treatment of B10C cells with BYL719 elicited a modest decrease in pAKT there was no effect on pPRAS40, pRPS6 or p4E-BP1. Most importantly, combined treatment of B10C cells with LGX818 plus BYL719 displayed no cooperative effects on pPRAS40, pRPS6 or p4E-BP1. Together, these data demonstrate that inhibition of PI3Kα enhanced the effects of $BRAF^{V600E}$ inhibition in $BRAF^{V600E}$/$PIK3CA^{H1047R}$ but not in $BRAF^{V600E}$/$PTEN^{Null}$ melanoma cells.

The anti-proliferative activity of PI3Kα selective inhibition on $BRAF^{V600E}$/$PIK3CA^{H1047R}$ cells *in vitro* prompted us to design a preclinical trial in mice to test the ability of BYL719, either alone or in combination with LGX818, to elicit regression of autochthonous $BRAF^{V600E}$/$PIK3CA^{H1047R}$ melanomas. To that end, $BRAF^{V600E}$/$PIK3CA^{H1047R}$ melanomas were initiated on the back skin of adult *Tyr::CreER; $BRaf^{CA}$; $Pik3ca^{lat/+}$* mice. In this scenario, melanomas are elicited by the cooperative action of two dominantly acting oncogenes: $BRAF^{V600E}$ and $PIK3CA^{H1047R}$ (11, 22). Seven weeks post-initiation (p.i), mice were randomized to receive vehicle, LGX818, BYL719, or combined LGX818 plus BYL719 treatment, with melanoma size measured weekly. Pharmacodynamic analysis of pAKT inhibition in $BRAF^{V600E}$/$PIK3CA^{H1047R}$ melanomas indicated the need to dose BYL719 twice daily to achieve maximal target inhibition (Fig. S1D).

Single agent BYL719 initially elicited modest melanoma regression (<30%), followed by a prolonged cytostatic effect (Fig. 1H). By contrast, single agent LGX818 elicited profound melanoma regression. Importantly, the combination of BYL719 plus LGX818 promoted significantly more potent melanoma regression than that observed with LGX818 monotherapy (Fig. 1H). Analysis of the best overall response by waterfall plot indicated that only 2/8 mice treated with BYL719 displayed >30% melanoma regression, which qualifies as a partial response (PR) by modified RECIST 1.1 guidelines (Fig. 1I) (23). By contrast, 7/7 mice treated with LGX818 exceeded the 30% regression threshold, as did 8/8 mice receiving BYL719+LGX818. Finally, combined treatment with LGX818 plus BYL719 provided significantly superior melanoma regression compared to single agent LGX818 therapy (Fig. 1I).

Analysis of glioblastoma, breast or prostate cancer models suggests that PI3′-kinase-β (PI3Kβ/PIK3CB) is the predominant driver of PI3′-lipid production in $PTEN^{Null}$ tumors (24, 25). Consequently, we tested the effects of PI3Kβ selective inhibition on the proliferation of human $BRAF^{V600E}$/$PTEN^{Null}$ melanoma-derived cells. Two structurally distinct PI3Kβ selective inhibitors were used: GSK2636771 (GSK771) and KIN193 (26–28). Perhaps surprisingly, even at the highest concentration tested (10μM), GSK771 failed to reach the GI_{50} of $BRAF^{V600E}$/$PTEN^{Null}$ human melanoma cells (Fig. 2A and Fig. S2A). Further, even at 5μM, GSK771 elicited only a minor reduction of pAKT in $BRAF^{V600E}$/$PTEN^{Null}$ melanoma cells, with no effects on the phosphorylation of downstream PI3K pathway components (Fig. 2B and Fig. S2B). While KIN193 displayed enhanced—but still modest—anti-proliferative activity compared to GSK771, the anti-proliferative activity of KIN193 on PI3Kα-dependent BPC cells (Fig. S2A) suggests that at higher concentrations, the anti-proliferative activity of KIN193 is likely due to inhibition of PI3Kα. Additionally, although

NIH-PA Author Manuscript

NIH-PA Author Manuscript

NIH-PA Author Manuscript

5μM KIN193 modestly suppressed pAKT in some human-derived $BRAF^{V600E}/PTEN^{Null}$ melanoma cells (Fig. 2B and S2B), the ability of 5μM KIN193 treatment to robustly suppress pAKT in PI3Kα-dependent BPC cells (Fig. S2B) further underscores the fact that this activity is likely due to inhibition of PI3Kα. B10C melanoma cells also displayed proliferative and biochemical resistance to PI3Kβ inhibition (Figs. S2A & S2B). Interestingly, while both KIN193 and GSK771 treatment suppressed pAKT activation in M249 $BRAF^{V600E}/PTEN^{Null}$ melanoma cells, this inhibition did not result in reduced phosphorylation of PRAS40 (Fig. S2B). Moreover, PI3Kβ inhibition had only modest anti-proliferative effects on M249 cells, suggesting that residual PI3Kβ-independent PI3K signaling was sufficient to sustain cell proliferation.

The lack of robust single agent activity on $BRAF^{V600E}/PTEN^{Null}$ melanoma cells observed with PI3Kβ selective inhibition led us to hypothesize that $BRAF^{V600E}/PTEN^{Null}$ human melanoma cells might require the combined activity of PI3Kα and PI3Kβ for sustained proliferation. To test this, we assessed cell proliferation of $BRAF^{V600E}/PTEN^{Null}$ cells treated with BYL719 in the presence or absence of a fixed concentration of GSK771 (Fig. 2C). Although PI3Kα inhibition had a modest inhibitory effect on melanoma cell proliferation, the addition of a PI3Kβ inhibitor did not dramatically enhance that effect, suggesting that $BRAF^{V600E}/PTEN^{Null}$ melanoma cells do not rely exclusively on the combined activity of PI3Kα and PI3Kβ for their proliferation.

To test if $BRAF^{V600E}/PTEN^{Null}$ melanoma cells require PI3Kβ to promote PI3′-lipid signaling with downstream effects on cell proliferation we employed GDC-0032, a PI3Kβ-sparing class I PI3K inhibitor that inhibits PI3Kα, δ and γ (29). Initially, we compared the anti-proliferative activity of GDC-0032 to that of GDC-0941, a pan-class I PI3K inhibitor (30). Both GDC-0032 and GDC-0941 displayed equivalent GI_{50} values in all $BRAF^{V600E}/PTEN^{Null}$ melanoma cells tested (Figs. 2D & S2C). Further, treatment with GDC-0032 elicited a dose-dependent reduction in pAKT and its downstream effectors with modestly enhanced potency compared to GDC-0941 (Figs. 2E & S2D). Taken together, these data indicate that PI3Kβ contributes little or nothing to PI3′-lipid signaling or proliferation of $BRAF^{V600E}/PTEN^{Null}$ melanoma cells.

To confirm that $BRAF^{V600E}/PTEN^{Null}$ melanoma cells rely on the combined activity of PI3Kα plus PI3Kδ and/or PI3Kγ for sustained proliferation, we investigated whether the effects of GDC-0032 could be mimicked by combined use of PI3Kα (BYL719) and PI3Kδ/γ (IPI145) selective inhibitors (31). Treatment of $BRAF^{V600E}/PTEN^{Null}$ WM793, 1205Lu or WM9 human melanoma cells with single agent BYL719 or IPI145 failed to reach the GI_{50}, even at 10μM (Fig. 2F). However, when the cells were treated with a fixed concentration of IPI145 (2.5μM) in the presence of BYL719, the combination elicited a more robust anti-proliferative response similar to the effects of GDC-0032 (Fig. 2F). Furthermore, while single agent treatment of WM9 cells with either BYL719 or IPI145 elicited only a modest reduction in pAKT with little or no effect on downstream pathway components, the combination of BYL719 plus IPI145 elicited a complete and sustained inhibition of pAKT that mirrored the effects of GDC-0032 (Fig. 2G). Similar results were obtained with 1205Lu $BRAF^{V600E}/PTEN^{Null}$ melanoma cells (Fig. S2E). Together, these results suggest that PI3Kβ activity is dispensable for the proliferation and PI3K pathway activation of

NIH-PA Author Manuscript

NIH-PA Author Manuscript

NIH-PA Author Manuscript

$BRAF^{V600E}/PTEN^{Null}$ melanoma cells and that these cells instead rely upon the combined activities of PI3Kα, δ and/or γ.

To determine if a PI3Kβ-sparing PI3K inhibitor might augment the effects of $BRAF^{V600E}$ pathway-targeted inhibition, we treated $BRAF^{V600E}/PTEN^{Null}$ human or mouse melanoma cells with GDC-0973 (an inhibitor of MEK1/2), GDC-0032, or GDC-0973 plus GDC-0032 (Figs. 3A & S3A) (32). Importantly, the combined use of these agents elicited robust suppression of pAKT and pERK, as well as more robust suppression of pRPS6 and p4EB-P1 than that achieved with either single agent alone. Additionally, whereas single agent GDC-0973 or GDC-0032 suppressed $BRAF^{V600E}/PTEN^{Null}$ human or mouse melanoma cell proliferation, combined treatment elicited a significant reduction in proliferation compared to either single agent alone (Figs. 3B & S3B).

The *in vitro* activity of GDC-0032 against $BRAF^{V600E}/PTEN^{Null}$ melanoma cells prompted us to conduct a preclinical trial to test the ability of GDC-0032 to elicit regression of $BRAF^{V600E}/PTEN^{Null}$ melanomas *in vivo*, either alone or in combination with GDC-0973. To that end, $BRAF^{V600E}/PTEN^{Null}$ melanoma was initiated in adult *Tyr::CreER; BRaf*^{CA}*; Pten*$^{lox/lox}$ mice and, seven weeks p.i., mice were randomized to receive vehicle, GDC-0973, GDC-0032 or combination therapy with melanoma size measured weekly (Fig. 3C). As with $BRAF^{V600E}/PIK3CA^{H1047R}$ melanomas treated with BYL719, inhibition of PI3K signaling with GDC-0032 had largely cytostatic effects on $BRAF^{V600E}/PTEN^{Null}$ melanomas (Figs. 3C & 3D). By contrast, MEK1/2 inhibition with GDC-0973 elicited substantial regression of $BRAF^{V600E}/PTEN^{Null}$ melanomas, which was significantly enhanced by combined treatment with GDC-0032 (Figs. 3C & 3D).

To investigate the potential role of PI3Kβ in *BRAF*-mutated melanoma cells in which there is no documented genetic alteration in components of PI3K signaling, we treated SK-MEL-239 human melanoma cells ($BRAF^{V600E}/PTEN^{WT}$) with inhibitors of PI3Kβ, and characterized the anti-proliferative response (Fig. S4A). While we observed modestly enhanced potency for KIN193 as compared to GSK771, the GI_{50} for both PI3Kβ inhibitors on SK-MEL-239 melanoma cells was >10μM. While SK-MEL-239 cells exhibit low basal levels of pAKT, inhibition of PI3Kβ did not suppress activation of downstream pathway components pPRAS40, pRPS6, or p4E-BP1 (Fig. S4B). Moreover, both GDC-0032 and GDC-0941 displayed equivalent GI_{50} values in SK-MEL-239 cells (Fig. S4C). The combined use of GDC-0032 plus GDC-0973 elicited robust suppression of pAKT and pERK, as well as an even more robust suppression of pRPS6 and p4E-BP1 than that achieved with either single agent (Fig. S4D). Finally, whereas single agent GDC-0973 or GDC-0032 suppressed SK-MEL-239 cell proliferation, combined treatment elicited a significant reduction in proliferation compared to either single agent alone (Figs. S4E). Collectively these results indicate that, in at least one $BRAF^{V600E}/PTEN^{WT}$ human melanoma cell line, PI3Kβ activity is dispensable for proliferation and that these cells rely upon the combined activities of PI3Kα, δ and/or γ.

Although the majority of *BRAF*-mutated melanoma patients experience initial tumor regression in response to $BRAF^{V600E}$ pathway-targeted therapies, the durability of response is limited by the onset of drug resistant disease (6). Therefore, we wished to test if inhibition

NIH-PA Author Manuscript

NIH-PA Author Manuscript

NIH-PA Author Manuscript

of class I PI3K isoform(s) would influence the development of resistance to inhibitors that target $BRAF^{V600E}$ signaling. We initially tested this question using vehicle-treated $BRAF^{V600E}/PTEN^{Null}$ melanoma-bearing mice enrolled in the study described in Fig. 3C. When these mice (n=8) were near to end-stage, they were randomly re-assigned to receive extended treatment with either GDC-0973 monotherapy or combined GDC-0973 plus GDC-0032. These mice received a reduced dose of GDC-0973 (2mg/kg) and a full dose GDC-0032 (22.5mg/kg) to minimize the toxicity of full dose combination therapy. As expected, mice in both treatment groups experienced initial tumor regression, which was superior with combined treatment compared to GDC-0973 monotherapy (Figs. 4A and 4B). However, over the course of 113 days of treatment, all of the mice receiving GDC-0973 monotherapy developed drug resistant disease, defined as tumor re-growth ≥100% of the tumor volume at the initiation of therapy. By contrast, none of the mice receiving combination therapy developed drug resistant disease. To further investigate the role of PI3K pathway activity in promoting resistance to GDC-0973 treatment, when the first mouse receiving GDC-0973 monotherapy reached end-stage, the tumor was resected, fragmented, and implanted into a cohort (n=8) of immunocompromised mice. Immediately following implantation, these mice received GDC-0973 monotherapy treatment. As expected, the transplanted tumor displayed resistance to GDC-0973 and grew progressively over 50 days. At this time, half of the mice were randomly re-assigned to receive GDC-0973 plus GDC-0032 combination therapy, while the rest continued to receive GDC-0973 monotherapy (Fig. 4C). The mice receiving GDC-0973 plus GDC-0032 combination therapy experienced potent tumor cytostasis, suggesting that PI3K pathway activity is necessary for the sustained growth of a melanoma that has developed resistance to a MEK1/2 inhibitor.

To further validate the ability of PI3K inhibitors to forestall the onset of resistance to targeted blockade of $BRAF^{V600E}$ signaling, $BRAF^{V600E}/PIK3CA^{H1047R/H1047R}$ melanoma was initiated in 13 adult *Tyr::CreER; BRaf^{CA}; Pik3ca$^{lat/lat}$* mice and, 61 days p.i., mice were randomized to receive GDC-0973 (2mg/kg) monotherapy or GDC-0973 plus BYL719 (50mg/kg) combination therapy. As observed with $BRAF^{V600E}/PTEN^{Null}$ driven melanomas, mice in both treatment groups experienced initial tumor regression, which was superior with combined treatment compared to GDC-0973 monotherapy (Figs. 4D and 4E). However, over the course of 106 days, 6/7 mice receiving GDC-0973 monotherapy developed drug resistant disease. By contrast, none of the mice receiving combination therapy developed drug resistance.

DISCUSSION

At the initiation of these studies, the high rate of *PTEN* silencing compared to mutational activation of *PIK3CA* suggested that PTEN might exert PI3′-lipid phosphatase-independent tumor suppressor functions to restrain progression of *BRAF*-mutated melanoma (14). We previously noted that, while heterozygous mutational activation of *Pik3ca^{lat}* was sufficient to promote melanoma progression, $BRAF^{V600E}/PIK3CA^{H1047R}$ melanomas grew significantly more slowly than did $BRAF^{V600E}/PTEN^{Null}$ melanomas (11). However, $BRAF^{V600E}$-driven melanomas homozygous for $PIK3CA^{H1047R}$ expression grew even more rapidly than $BRAF^{V600E}/PTEN^{Null}$ melanomas. Although we cannot formally exclude a role

NIH-PA Author Manuscript

NIH-PA Author Manuscript

NIH-PA Author Manuscript

for PI3′-lipid phosphatase-independent PTEN tumor suppressor functions to restrain progression of *BRAF*-mutated melanoma, there is no compelling rationale to invoke such mechanisms. Importantly, the correlation between PI3K pathway activation and melanoma growth rate indicates that PI3K catalytic isoforms are relevant drug targets in the treatment of $BRAF^{V600E}/PTEN^{Null}$ melanoma.

The “oncogene addiction” hypothesis posits that, despite a high burden of genetic damage, tumors remain dependent on the sustained activity of one or a small number of oncogenes for maintenance of the malignant phenotype (33). As a corollary, inhibition of the oncogene(s) to which a tumor is addicted can elicit profound tumor regression (34). Accordingly, our model of $BRAF^{V600E}/PIK3CA^{H1047R}$ melanoma is driven by two oncogene activation events one of which, $BRAF^{V600E}$, drives tumor initiation and the other of which, $PIK3CA^{H1047R}$, promotes melanoma progression (22). Potent inhibitors of either $BRAF^{V600E}$ or $PIK3CA^{H1047R}$ allowed us to characterize to which of these two oncoproteins are $BRAF^{V600E}/PIK3CA^{H1047R}$ melanomas most addicted *in vivo*. While inhibition of $BRAF^{V600E}$ elicited profound melanoma regression, selective inhibition of $PIK3CA^{H1047R}$ elicited largely cytostatic effects: only 2/8 mice displayed a ≥30% reduction in melanoma size in response to BYL719 monotherapy and that response was largely transient (23). These results may illustrate a fundamental difference between the effects of oncogenic $BRAF^{V600E}$ and $PIK3CA^{H1047R}$ on the sustained survival of melanoma cells, carrying potential clinical implications.

Previous studies of PTEN deficient tumor cells have indicated that PI3Kβ is an essential contributor to PI3′-lipid signaling and aberrant cell proliferation (24, 25). However, our work suggests that PI3Kβ, either alone or in combination with PI3Kα, does not contribute to PI3′-lipid signaling or to the proliferation of human or mouse $BRAF^{V600E}/PTEN^{Null}$ melanoma cells. Although PI3Kβ inhibitors modestly attenuated pAKT in M249 cells, this did not translate into suppression of cell proliferation. Furthermore, a PI3Kβ–sparing inhibitor and a combination of agents that inhibits PI3Kα, δ and γ had potent inhibitory effects on PI3′-lipid signaling and proliferation of $BRAF^{V600E}/PTEN^{Null}$ melanoma cells. Interestingly, SK-MEL-239 melanoma cells, which express $BRAF^{V600E}$ and normal PTEN, also displayed resistance to PI3Kβ inhibition and equivalent sensitivity to pan class I (GDC-0941) or PI3Kβ-sparing PI3K inhibition (GDC-0032), demonstrating no role for PI3Kβ in these cells. It is tempting to speculate that PI3Kβ may play a role in the proliferation of melanomas in which *RAC1* is mutated or amplified, as PI3Kβ is a direct target of activated RAC1-GTP (1, 35).

Despite the potent biochemical and anti-proliferative effects of the PI3Kβ-sparing inhibitor GDC-0032 *in vitro*, this agent elicited largely cytostatic effects in our $BRAF^{V600E}/PTEN^{Null}$ GEM melanoma model and showed modest, but significant, cooperation with MEK1/2 inhibition to promote melanoma regression. Perplexingly, although both human and mouse cancer genetics indicate an important role for PI3K signaling in disease progression, the limited activity of PI3K inhibitors in solid tumor clinical trials does not correlate with PI3K pathway activation (36). This may be due to a role for PI3K signaling predominantly in promoting cell cycle progression and not for suppression of apoptosis. However, more promisingly, treatment with GDC-0032 forestalled the onset of resistance to a MEK1/2

NIH-PA Author Manuscript

NIH-PA Author Manuscript

NIH-PA Author Manuscript

inhibitor (GDC-0973) in our GEM model of $BRAF^{V600E}$/$PTEN^{Null}$ melanoma. Importantly, upon serial transplantation, MEK1/2 inhibitor resistant melanomas retained sensitivity to combined GDC-0973 plus GDC-0032 treatment, highlighting the importance of PI3K pathway signaling in maintenance of the MEK1/2 inhibitor-resistant phenotype. Further emphasizing the importance of PI3K signaling in MEK1/2 inhibitor resistance, the emergence of GDC-0973 resistant melanomas was forestalled by combined treatment with BYL719 in our $BRAF^{V600E}$/$PIK3CA^{H1047R}$ GEM melanoma model. Since a major limitation in single agent treatment of *BRAF*-mutated melanoma is the onset of drug resistant disease, the observation that PI3K inhibition enhances the depth and durability of response to $BRAF^{V600E}$ pathway-targeted inhibition may illuminate an arena in which PI3K inhibitors will offer substantial clinical benefit.

MATERIALS AND METHODS

Cell Culture and Drug Treatments

Human melanoma cell lines WM793, WM9, and 1205Lu were kindly provided from the well-curated cell line repository established by Dr. Meenhard Herlyn (Wistar Institute, Philadelphia, PA), and genomic sequencing of these cells was performed in the laboratory of Dr. Katherine Nathanson (University of Pennsylvania, Philadelphia, PA). Human melanoma cell lines M249 and M233 were kindly provided by Dr. Antoni Ribas (University of California, Los Angeles, Los Angeles, CA) and authenticated by genomic sequencing as previously described (37). Human melanoma cell line SK-MEL-239 was kindly provided by Dr. David B. Solit (Memorial Sloan-Kettering Cancer Center, New York, NY) authenticated by genomic sequencing as previously described (38). Mouse melanoma cell lines B10C, BPC, and BP_2C were established as described previously and authenticated by PCR and immunoblot analyses (11). Efficient generation of melanoma cell lines from our various GEM models requires the silencing of the *Cdkn2a* locus encoding INK4A and ARF. Mouse or human melanoma cell lines were cultured as described previously (11). Pathway-targeted pharmacological agents were obtained from various colleagues in the public or private sector or from commercial sources (see Supplementary Table 1 for provenance).

Proliferation and Growth Assays

Melanoma cell proliferation was assessed over 72-hours by seeding 5×10^4 cells in 12-well dishes. Cells were treated with the various pharmacological agents as described with viable cells enumerated using a Countess® cell counter (Invitrogen). In addition, melanoma cells were seeded and treated with pharmacological agents as described for 72 hours at which time viable cells were stained with crystal violet and quantified by solubilization in 33% acetic acid with A562 absorbance assessed. GI_{50} assays were performed by seeding 8.0×10^3 cells in a 96-well plate and treating cells with pharmacological agents as described for 72 hours at which time viable cells were stained with Crystal Violet and quantified by solubilization in 33%(v/v) acetic acid with A562 absorbance assessed. At least three independent experiments, performed in biological triplicate, were completed for all 72-hour assays. Long-term colony formation assays were performed by culturing 500–2000 cells in a 10cm dish for 6–11 days in the absence or presence of various agents with cell colonies fixed and stained with Crystal Violet.

NIH-PA Author Manuscript

NIH-PA Author Manuscript

NIH-PA Author Manuscript

Immunoblot Analysis

Cell lysates were generated for analysis of 50μg aliquots by immunoblotting as described previously (20). Membranes were stained with primary antibodies with antigen-antibody complexes detected using fluorescent goat anti-Rabbit IRDye 800 or goat anti-Mouse IRDye 680 secondary antibodies (LI-COR Biosciences) and visualized with a LI-COR infrared imaging system (Odyssey Fc). Immunoblot data were analyzed using Image Studio v2.0 software (LI-COR Biosciences).

Experimental Animals

The UCSF Institutional Animal Care and Use Committee (IACUC) reviewed and approved all animal procedures. *Tyr::CreER*, *BRaf*^{CA}, *Pten*$^{lox4-5}$ or *Pik3ca*$^{Lat-1047R}$ mice, maintained on an outbred background, were intercrossed to generate experimental mice which were genotyped as previously described (11, 12). Melanocyte-specific Cre activity was induced in adult mice by topical application of 1.5μl of 5mM 4-hydroxytamoxifen (4-HT, 70% Z-isomer, in 100% Ethanol, Sigma Aldrich) to shaved back skin. Animals were euthanized based on a body conditioning score (39) or when tumor volume ≥2cm^3, whichever occurred first. At necropsy, tissue was snap frozen in liquid nitrogen. Tissue was homogenized in RIPA buffer using the Tissue Lyser II (Qiagen®) for immunoblotting as described previously (11).

Treatment of Mice with Pathway-Targeted Inhibitors

Melanoma-bearing mice were divided among treatment arms to give equal distribution of tumor volume and gender when the mean tumor volume of the cohort exceeded 500mm^3. Mice were assigned to receive LGX818 (30mg/kg q.d.) or BYL719 (50mg/kg b.i.d.) formulated in 0.5%(w/v) carboxymethylcellulose/0.5%(v/v) Tween-80 (Sigma Aldrich) or GDC-0973 (2.0 or 4.5mg/kg q.d.) or GDC-0032 (22.5mg/kg q.d.) formulated in 0.5%(w/v) methylcellulose/0.2%(v/v) Tween-80 (Sigma Aldrich) and administered via oral gavage six days per week. Melanoma growth was measured weekly using digital calipers with relative tumor volume (RTV) estimated using the ellipsoid volume formula as described previously (11).

Statistical Analysis

All quantitative data is represented as means ± SEM. GraphPad Prism 6 statistical software was used to determine *p* values for the proliferation graphs by performing two-way ANOVA analysis and *t*-tests as indicated.

Supplementary Material

Refer to Web version on PubMed Central for supplementary material.

Acknowledgments

We thank all of the members of the McMahon lab for advice and guidance on this project, with special thanks to Jillian Silva for stimulating discussions on melanoma cell signaling and immunoblotting. We thank Adil Daud (UCSF) for invigorating discussions on melanoma therapy, Meenhard Herlyn (Wistar Institute) and Antoni Ribas (UCLA) for melanoma cell lines and Marcus Bosenberg (Yale School of Medicine) for *Tyr::CreER* mice. We thank colleagues for providing access to the following compounds and information on their use: Emmanuelle Di Tomaso,

NIH-PA Author Manuscript

NIH-PA Author Manuscript

NIH-PA Author Manuscript

Janet Lyle, and Darrin Stuart (Novartis) for BYL719 and LGX818 and Leisa Johnson, Deepak Sampath and Lori Freedman (Genentech) for GDC-0941, GDC-0032 and GDC-0973 (Genentech). We thank Byron Hann and the Helen Diller Family Comprehensive Cancer Center's Preclinical Therapeutics Core for advice and the Laboratory Animal Resource Center for animal husbandry. We thank the mice for their participation. This research was supported by grants from the National Health and Medical Research Council of Australia (to WAP) and the National Cancer Institute (CA176839), Melanoma Research Alliance & National Comprehensive Cancer Network (to MM).

References

1. Hodis E, Watson IR, Kryukov GV, Arold ST, Imielinski M, Theurillat JP, et al. A landscape of driver mutations in melanoma. Cell. 2012; 150:251–63. [PubMed: 22817889]
2. Bastian BC. The molecular pathology of melanoma: an integrated taxonomy of melanocytic neoplasia. Annu Rev Pathol. 2014; 9:239–71. [PubMed: 24460190]
3. Davies H, Bignell GR, Cox C, Stephens P, Edkins S, Clegg S, et al. Mutations of the BRAF gene in human cancer. Nature. 2002; 417:949–54. [PubMed: 12068308]
4. McArthur GC, Robert PBC, et al. Improved survival with vemurafenib in BRAFV600E and BRAFV600K mutation-positive melanoma. Lancet Oncol. 2014 In Press.
5. Hauschild A, Grob JJ, Demidov LV, Jouary T, Gutzmer R, Millward M, et al. Dabrafenib in BRAF-mutated metastatic melanoma: a multicentre, open-label, phase 3 randomised controlled trial. Lancet. 2012; 380:358–65. [PubMed: 22735384]
6. Holderfield M, Deuker MM, McCormick F, McMahon M. Targeting RAF kinases for cancer therapy: BRAF-mutated melanoma and beyond. Nature reviews Cancer. 2014; 14:455–67.
7. Lito P, Rosen N, Solit DB. Tumor adaptation and resistance to RAF inhibitors. Nat Med. 2013; 19:1401–9. [PubMed: 24202393]
8. Bucheit AD, Davies MA. Emerging insights into resistance to BRAF inhibitors in melanoma. Biochem Pharmacol. 2014; 87:381–9. [PubMed: 24291778]
9. Shi H, Hugo W, Kong X, Hong A, Koya RC, Moriceau G, et al. Acquired resistance and clonal evolution in melanoma during BRAF inhibitor therapy. Cancer Discov. 2014; 4:80–93. [PubMed: 24265155]
10. Nazarian R, Shi H, Wang Q, Kong X, Koya RC, Lee H, et al. Melanomas acquire resistance to B-RAF(V600E) inhibition by RTK or N-RAS upregulation. Nature. 2010; 468:973–7. [PubMed: 21107323]
11. Marsh Durban V, Deuker MM, Bosenberg MW, Phillips W, McMahon M. Differential AKT dependency displayed by mouse models of BRAFV600E-initiated melanoma. J Clin Invest. 2013; 123:5104–18. [PubMed: 24200692]
12. Dankort D, Curley DP, Cartlidge RA, Nelson B, Karnezis AN, Damsky WE Jr, et al. Braf(V600E) cooperates with Pten loss to induce metastatic melanoma. Nat Genet. 2009; 41:544–52. [PubMed: 19282848]
13. Tsao H, Goel V, Wu H, Yang G, Haluska FG. Genetic interaction between NRAS and BRAF mutations and PTEN/MMAC1 inactivation in melanoma. J Invest Dermatol. 2004; 122:337–41. [PubMed: 15009714]
14. Shull AY, Latham-Schwark A, Ramasamy P, Leskoske K, Oroian D, Birtwistle MR, et al. Novel somatic mutations to PI3K pathway genes in metastatic melanoma. PLoS One. 2012; 7:e43369. [PubMed: 22912864]
15. Kim JE, Stones C, Joseph WR, Leung E, Finlay GJ, Shelling AN, et al. Comparison of growth factor signalling pathway utilisation in cultured normal melanocytes and melanoma cell lines. BMC Cancer. 2012; 12:141. [PubMed: 22475322]
16. Shen WH, Balajee AS, Wang J, Wu H, Eng C, Pandolfi PP, et al. Essential role for nuclear PTEN in maintaining chromosomal integrity. Cell. 2007; 128:157–70. [PubMed: 17218262]
17. Song MS, Carracedo A, Salmena L, Song SJ, Egia A, Malumbres M, et al. Nuclear PTEN regulates the APC-CDH1 tumor-suppressive complex in a phosphatase-independent manner. Cell. 2011; 144:187–99. [PubMed: 21241890]
18. Wu H, Goel V, Haluska FG. PTEN signaling pathways in melanoma. Oncogene. 2003; 22:3113–22. [PubMed: 12789288]

NIH-PA Author Manuscript NIH-PA Author Manuscript NIH-PA Author Manuscript

19. Furet P, Guagnano V, Fairhurst RA, Imbach-Weese P, Bruce I, Knapp M, et al. Discovery of NVP-BYL719 a potent and selective phosphatidylinositol-3 kinase alpha inhibitor selected for clinical evaluation. Bioorg Med Chem Lett. 2013; 23:3741–8. [PubMed: 23726034]
20. Silva JM, Bulman C, McMahon M. BRAFV600E cooperates with PI3K signaling, independent of AKT, to regulate melanoma cell proliferation. Mol Cancer Res. 2014; 12:447–63. [PubMed: 24425783]
21. Darrin D, Stuart NL, Poon Daniel J, Aardalen Kimberly, Kaufman Susan, Merritt Hanne, Salangsang Fernando, Lorenzana Edward, Li Allen, Ghoddusi Majid, Caponigro Giordano, Sun Frank, Kulkarni Swarupa, Kakar Shefali, Turner Nancy, Zang Richard, Tellew John, Pryer Nancy. Preclinical profile of LGX818: A potent and selective RAF kinase inhibitor. Cancer Res. 2012:72.
22. Vredeveld LC, Possik PA, Smit MA, Meissl K, Michaloglou C, Horlings HM, et al. Abrogation of BRAFV600E-induced senescence by PI3K pathway activation contributes to melanomagenesis. Genes Dev. 2012; 26:1055–69. [PubMed: 22549727]
23. Eisenhauer EA, Therasse P, Bogaerts J, Schwartz LH, Sargent D, Ford R, et al. New response evaluation criteria in solid tumours: revised RECIST guideline (version 1.1). Eur J Cancer. 2009; 45:228–47. [PubMed: 19097774]
24. Wee S, Wiederschain D, Maira SM, Loo A, Miller C, deBeaumont R, et al. PTEN-deficient cancers depend on PIK3CB. Proc Natl Acad Sci U S A. 2008; 105:13057–62. [PubMed: 18755892]
25. Jia S, Liu Z, Zhang S, Liu P, Zhang L, Lee SH, et al. Essential roles of PI(3)K-p110beta in cell growth, metabolism and tumorigenesis. Nature. 2008; 454:776–9. [PubMed: 18594509]
26. Jackson SP, Schoenwaelder SM, Goncalves I, Nesbitt WS, Yap CL, Wright CE, et al. PI 3-kinase p110beta: a new target for antithrombotic therapy. Nat Med. 2005; 11:507–14. [PubMed: 15834429]
27. Ralph A, Rivero MAH. Identification of GSK2636771, a potent and selective, orally bioavailable inhibitor of phosphatidylinositol 3-kinase-beta (PI3Kα) for the treatment of PTEN deficient tumors. Cancer Res. 2012:72.
28. Ni J, Liu Q, Xie S, Carlson C, Von T, Vogel K, et al. Functional characterization of an isoform-selective inhibitor of PI3K-p110beta as a potential anticancer agent. Cancer Discov. 2012; 2:425–33. [PubMed: 22588880]
29. Ndubaku CO, Heffron TP, Staben ST, Baumgardner M, Blaquiere N, Bradley E, et al. Discovery of 2-{3-[2-(1-isopropyl-3-methyl-1H-1,2-4-triazol-5-yl)-5,6-dihydrobenzo[f]imidazo[1,2-d][1,4]oxazepin-9-yl]-1H-pyrazol-1-yl}-2-methylpropanamide (GDC-0032): a beta-sparing phosphoinositide 3-kinase inhibitor with high unbound exposure and robust in vivo antitumor activity. J Med Chem. 2013; 56:4597–610. [PubMed: 23662903]
30. Folkes AJ, Ahmadi K, Alderton WK, Alix S, Baker SJ, Box G, et al. The identification of 2-(1H-indazol-4-yl)-6-(4-methanesulfonyl-piperazin-1-ylmethyl)-4-morpholin-4-yl-t hieno[3,2-d]pyrimidine (GDC-0941) as a potent, selective, orally bioavailable inhibitor of class I PI3 kinase for the treatment of cancer. J Med Chem. 2008; 51:5522–32. [PubMed: 18754654]
31. Winkler DG, Faia KL, DiNitto JP, Ali JA, White KF, Brophy EE, et al. PI3K-delta and PI3K-gamma inhibition by IPI-145 abrogates immune responses and suppresses activity in autoimmune and inflammatory disease models. Chem Biol. 2013; 20:1364–74. [PubMed: 24211136]
32. Rice KD, Aay N, Anand NK, Blazey CM, Bowles OJ, Bussenius J, et al. Novel Carboxamide-Based Allosteric MEK Inhibitors: Discovery and Optimization Efforts toward XL518 (GDC-0973). ACS Med Chem Lett. 2012; 3:416–21. [PubMed: 24900486]
33. Weinstein IB. Cancer. Addiction to oncogenes--the Achilles heal of cancer. Science. 2002; 297:63–4. [PubMed: 12098689]
34. Weinstein IB, Joe A. Oncogene addiction. Cancer Res. 2008; 68:3077–80. discussion 80. [PubMed: 18451130]
35. Fritsch R, de Krijger I, Fritsch K, George R, Reason B, Kumar MS, et al. RAS and RHO families of GTPases directly regulate distinct phosphoinositide 3-kinase isoforms. Cell. 2013; 153:1050–63. [PubMed: 23706742]

NIH-PA Author Manuscript

NIH-PA Author Manuscript

NIH-PA Author Manuscript

36. Rodon J, Brana I, Siu LL, De Jonge MJ, Homji N, Mills D, et al. Phase I dose-escalation and -expansion study of buparlisib (BKM120), an oral pan-Class I PI3K inhibitor, in patients with advanced solid tumors. Invest New Drugs. 2014; 32:670–81. [PubMed: 24652201]

37. Sondergaard JN, Nazarian R, Wang Q, Guo D, Hsueh T, Mok S, et al. Differential sensitivity of melanoma cell lines with BRAFV600E mutation to the specific Raf inhibitor PLX4032. Journal of translational medicine. 2010; 8:39. [PubMed: 20406486]

38. Poulikakos PI, Persaud Y, Janakiraman M, Kong X, Ng C, Moriceau G, et al. RAF inhibitor resistance is mediated by dimerization of aberrantly spliced BRAF(V600E). Nature. 2011; 480:387–90. [PubMed: 22113612]

39. Ullman-Cullere MH, Foltz CJ. Body condition scoring: a rapid and accurate method for assessing health status in mice. Lab Anim Sci. 1999; 49:319–23. [PubMed: 10403450]

NIH-PA Author Manuscript

NIH-PA Author Manuscript

NIH-PA Author Manuscript

STATEMENT OF SIGNIFICANCE

Although $BRAF^{V600E}$ pathway-targeted therapies elicit melanoma regression, the onset of drug resistance limits the durability of response. Here we show that combined treatment with PI3K inhibitors significantly forestalled the onset of MEK1/2 inhibitor resistant disease in *BRAF*-mutated GEM melanoma models. These results provide a conceptual framework for the combined deployment of $BRAF^{V600E}$ plus PI3K pathway-targeted inhibitors in the treatment of a subset of *BRAF*-mutated melanoma patients.

NIH-PA Author Manuscript

NIH-PA Author Manuscript

NIH-PA Author Manuscript

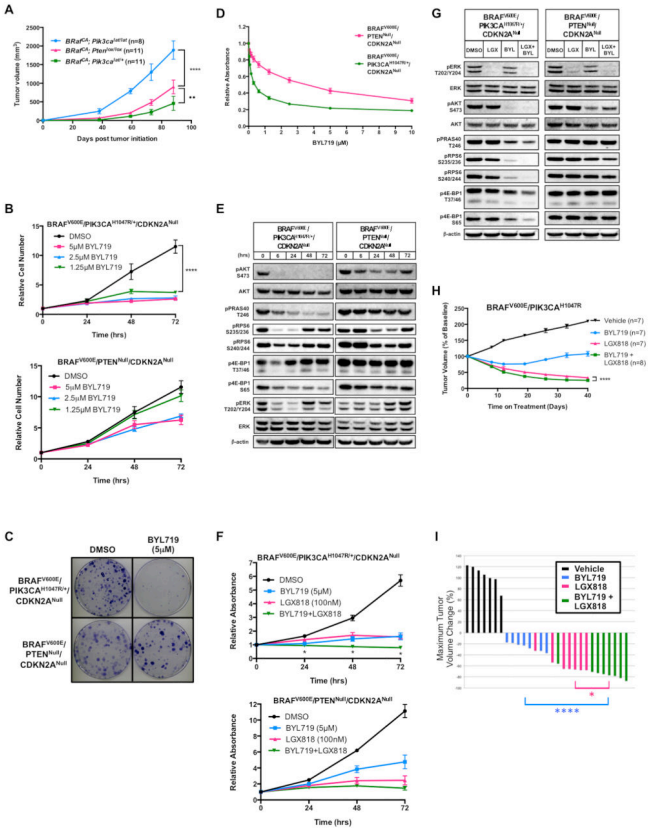

Figure 1. Autochthonous BRAF^{V600E}/PIK3CA^{H1047R} melanomas and cell lines are sensitive to PI3Kα-selective inhibition

(A) Melanoma was initiated in *Tyr::CreER; BRaf^{CA}* mice carrying *Pten$^{lox/lox}$* or either heterozygous or homozygous for *Pik3ca^{lat}* by topical application of 4-hydroxytamoxifen (4-HT), with melanoma growth assessed for 88 days. Average tumor volumes (mm^3 ± SEM) were measured starting at day 38 days p.i. Asterisks indicate significant difference in melanoma growth between *Tyr::CreER; BRaf^{CA}; Pik3ca$^{lat/lat}$* and *Tyr::CreER; BRaf^{CA}; Pten$^{lox/lox}$* mice and filled circles indicate significant difference between *Tyr::CreER; BRaf^{CA}; Pik3ca$^{lat/+}$* and *Tyr::CreER; BRaf^{CA}; Pten$^{lox/lox}$* mice (2-way ANOVA, ••, *p<0.005*, ****, *p<0.0001*).

(B) BPC or B10C melanoma cells were cultured in the presence of the indicated concentrations of BYL719 with cells counted every 24 hours for 72 hours. Cell counts are indicated as change in cell number relative to the number of cells at the initiation of drug treatment with error bars representing standard error of the mean (SEM). Asterisks indicate significant difference between DMSO and 1.25μM BYL719 (2-way ANOVA, *p<0.0001*).

(C) BPC or B10C melanoma cells were cultured in the presence of BYL719 (5μM) for a period of nine days before being fixed and stained with Crystal Violet.

(D) BPC or B10C melanoma cells were cultured in the presence of the indicated concentrations of BYL719 for 72 hours before being fixed and stained with Crystal Violet. Crystal Violet staining was quantified by solubilizing the fixed dye and assessing the absorbance at 562nm. Values are normalized to DMSO control and error bars represent SEM.

NIH-PA Author Manuscript

NIH-PA Author Manuscript

NIH-PA Author Manuscript

(E) Lysates of BPC or B10C melanoma cells, treated for the indicated period of time with BYL719 (5μM), were analyzed by immunoblotting with the indicated antisera.
(F) BPC or B10C melanoma cells were cultured in the presence of BYL719 (5μM), LGX818 (100nM) or the combination of both agents with cells fixed and stained with Crystal Violet every 24 hours for a total period of 72 hours. Crystal Violet staining was quantified as described above. Error bars represent SEM. Asterisks indicate significant difference between combination drug treatment and LGX818 treatment (multiple *t*-tests, $p<0.05$).
(G) Lysates of BPC or B10C melanoma cells treated for 6 hours with DMSO, LGX818 (100nM), BYL719 (5μM) or the combination of both agents were analyzed by immunoblotting.
(H) $BRAF^{V600E}$/$PIK3CA^{H1047R}$ melanomas were initiated in suitably manipulated adult *Tyr::CreER*, $BRaf^{CA}$; $Pik3ca^{lat}$ mice. Following randomization, mice were treated with vehicle, BYL719 (50mg/kg, b.i.d.), LGX818 (30mg/kg, q.d.) or the combination of both agents. Melanoma growth or regression was measured weekly with digital calipers over the course of 40 days of continuous drug treatment. Tumor sizes are displayed as the average percent change in tumor size from the start of treatment, with error bars indicating SEM. Asterisks indicate significant difference between combination drug treatment and LGX818 drug treatment (2-way ANOVA, $p<0.0001$).
(I) A waterfall plot of the best tumor response for each of the 29 mice that received vehicle versus drug treatment in (H). The percent change in tumor size from the start of treatment is shown on the *y*-axis. Negative values indicate tumor shrinkage. Asterisks indicate significant difference between combination drug treatment and BYL719 (blue) or LGX818 (pink) (Unpaired *t*-test, *, $p<0.05$, ****, $p<0.0001$).

NIH-PA Author Manuscript

NIH-PA Author Manuscript

NIH-PA Author Manuscript

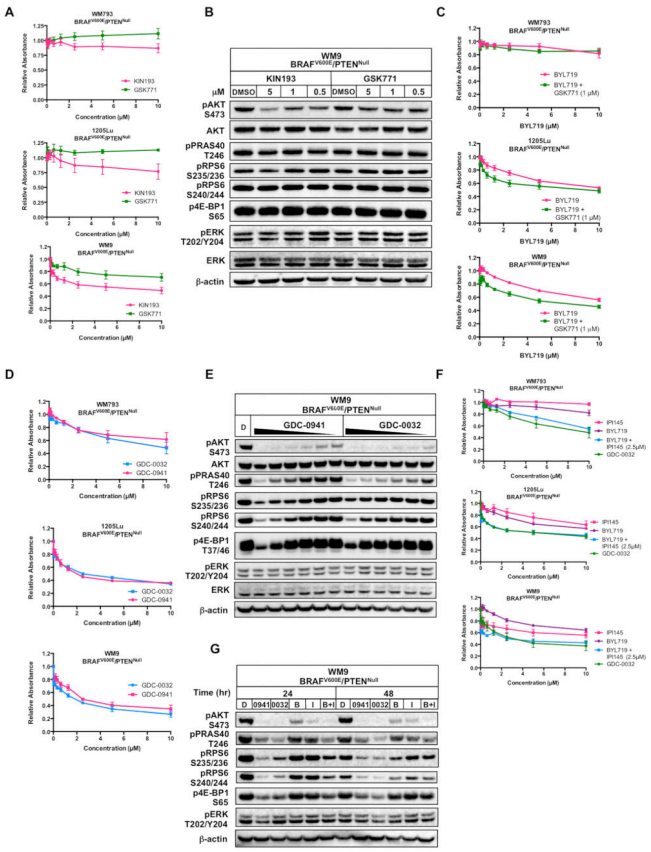

Figure 2. BRAF^{V600E}/PTEN^{Null} human melanoma-derived cells are insensitive to PI3Kβ-selective inhibition but sensitive to PI3Kβ-sparing class I PI3K inhibition

(A) WM793, 1205Lu or WM9 melanoma cells were cultured in the presence of the indicated concentrations of KIN193 (pink) or GSK771 (green) for 72 hours before being fixed and stained with Crystal Violet. Crystal Violet staining was quantified as described above. Values indicated are normalized to DMSO control and error bars represent SEM.

(B) Lysates of WM9 melanoma cells treated for 24 hours with the indicated concentrations of KIN193 or GSK771 were analyzed by immunoblotting.

(C) WM793, 1205Lu or WM9 melanoma cells were cultured in the presence of the indicated concentrations of BYL719 (pink) or BYL719 plus GSK771 (1μM, green) for 72 hours prior to fixation and staining with Crystal Violet. Crystal Violet staining was quantified as described above. Values indicated are normalized to DMSO control and error bars represent SEM.

(D) WM793, 1205Lu or WM9 melanoma cells were cultured in the presence of the indicated concentrations of GDC-0032 (blue) or GDC-0941 (pink) for 72 hours prior to fixation and staining with Crystal Violet. Crystal Violet staining was quantified as described above. Values indicated are normalized to DMSO control and error bars represent SEM.

(E) Lysates of WM9 melanoma cells, treated for 24 hours with DMSO (D), GDC-0941 or GDC-0032, with drug treatment applied in a serial two-fold dilution series from 10μM to 31.25 nM as indicated by gradient, were analyzed by immunoblotting.

(F) WM793, 1205Lu or WM9 melanoma cells were cultured in the presence of the indicated concentrations of IPI145 (pink), BYL719 (purple), BYL719 + 2.5μM IPI145 (blue) or

GDC-0032 (green) for 72 hours prior to fixation and staining with Crystal Violet. Crystal Violet staining was quantified as described above. Values indicated are normalized to DMSO control and error bars represent SEM.

(G) Lysates of WM9 melanoma cells treated for the indicated time period with DMSO (D), GDC-0941 (0941), GDC-0032 (0032), BYL719 (B), IPI145 (I) or BYL719+IPI145 (B+I) (all at 5μM) were analyzed by immunoblotting.

NIH-PA Author Manuscript
NIH-PA Author Manuscript
NIH-PA Author Manuscript

NIH-PA Author Manuscript
NIH-PA Author Manuscript
NIH-PA Author Manuscript

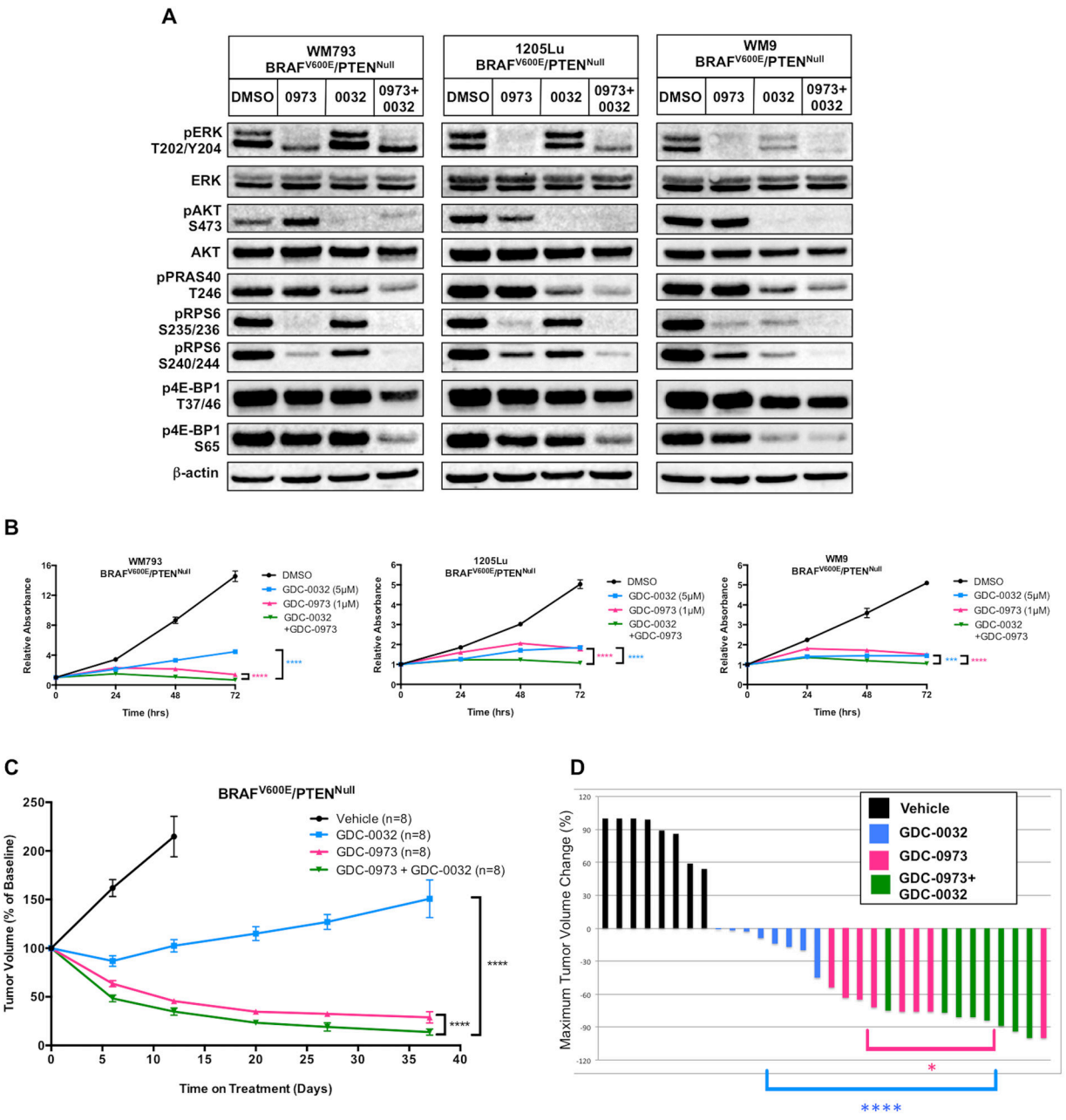

Figure 3. A PI3Kβ-sparing inhibitor enhances the effects of MEK1/2 inhibition on both BRAF^{V600E}/PTEN^{Null} human melanoma cells and autochthonous mouse melanomas

(A) Lysates of WM793, 1205Lu or WM9 melanoma cells treated for 6 hours with DSMO, GDC-0973 (1μM, 0973), GDC-0032 (5μM, 0032) or GDC-0973 plus GDC-0032 (0973+0032) were analyzed by immunoblotting.

(B) WM793, 1205Lu or WM9 melanoma cells were cultured in the presence of GDC-0032 (5μM, blue), GDC-0973 (1μM, pink) or GDC-0973 plus GDC-0032 (green) with cells fixed and stained with Crystal Violet every 24 hours for of 72 hours. Crystal Violet staining was quantified as described above. Error bars represent SEM. Asterisks indicate significant

NIH-PA Author Manuscript

NIH-PA Author Manuscript

NIH-PA Author Manuscript

difference between combination drug treatment and single agent drug treatment (2-way ANOVA, ***, *p<0.0005*, ****, *p<0.0001*).

(C) $BRAF^{V600E}/PTEN^{Null}$ melanomas were initiated in suitably manipulated adult *Tyr::CreER, $BRaf^{CA}$; $Pten^{lox/lox}$* mice. Following randomization, mice were treated with vehicle, single agent or combination GDC-0032 (22.5mg/kg) and GDC-0973 (4.5mg/kg, q.d.). Melanoma growth or regression was measured weekly with digital calipers over the course of 37 days of continuous drug treatment. Mice received GDC-0032 (as single agent or combination therapy) on a b.i.d. regimen for the first 12 days of treatment, but due to apparent toxicity, mice were dosed q.d starting on day 13. Tumor sizes are displayed as the average percent change in tumor size from the start of treatment, with error bars indicating SEM. Asterisks indicate significant difference between combination drug treatment and single agent drug treatment (2-way ANOVA, *p<0.0001*).

(D) A waterfall plot of the best tumor response for each of the 32 mice that received vehicle versus drug treatment in (C). The percent change in tumor size from the start of treatment is shown on the *y*-axis. Negative values indicate tumor shrinkage. Asterisks indicate significant difference between combination drug treatment and GDC-0032 (blue) or GDC-0973 (pink) (Unpaired *t*-test, *, *p<0.05*, ****, *p<0.0001*).

NIH-PA Author Manuscript
NIH-PA Author Manuscript
NIH-PA Author Manuscript

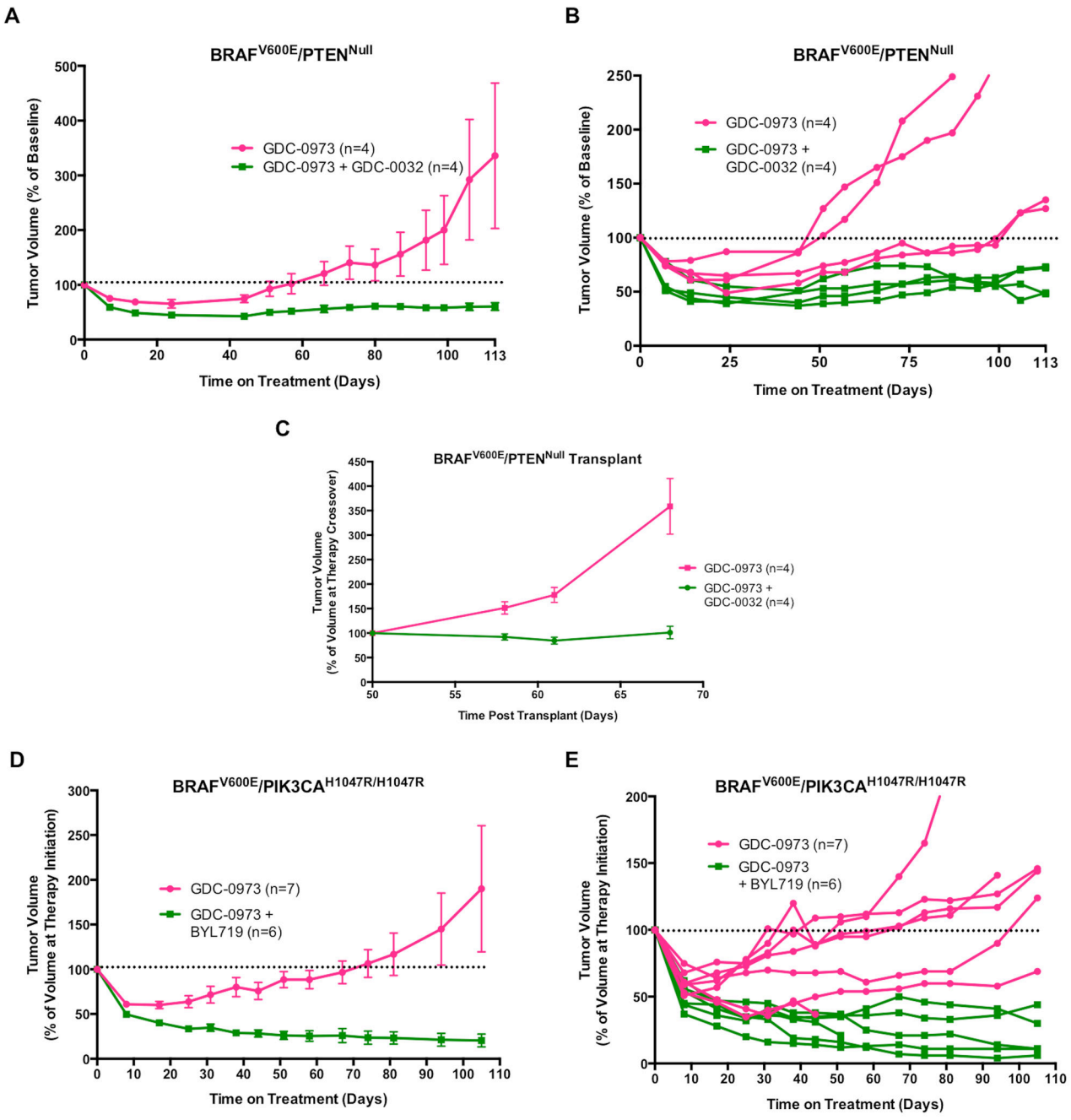

Figure 4. PI3K inhibition forestalls the development of MEK1/2 inhibitor resistance in two different GEM models of melanoma

(A) After two weeks of vehicle treatment, BRAF^{V600E}/PTEN^{Null} melanoma-bearing mice from the experiment described in Fig. 3C were crossed over to receive either GDC-0973 (2mg/kg) or GDC-0973 (2mg/kg) plus GDC-0032 (22.5mg/kg). Tumors were measured weekly with digital calipers with tumor size displayed as the average percent change in tumor size from the initiation of drug treatment, with error bars indicating SEM.

(B) A spider plot of the individual tumor response for each of the eight mice treated in **(E)**. Horizontal dotted line indicates progressive disease when tumor volume was ≥100% of

NIH-PA Author Manuscript

NIH-PA Author Manuscript

NIH-PA Author Manuscript

tumor volume prior to drug treatment. Tumor sizes are displayed as the average percent change in tumor size from the crossover point.

(C) Fragments of a single GDC-0973 resistant tumor from (A) were implanted into eight immunocompromised mice and allowed to grow into measurable tumors over 50 days with daily administration of GDC-0973 (2mg/kg). At that time, mice were randomized to receive either combination GDC-0973 (2mg/kg) plus GDC-0032 (22.5mg/kg) (green) or continuation of single agent GDC-0973 (2mg/kg) (pink). Tumor sizes were measured weekly and plotted as described previously. Tumor sizes are displayed as the average percent change in tumor size from the crossover point, with error bars indicating SEM.

(D) $BRAF^{V600E}$/$PIK3CA^{H1047R}$ melanomas were initiated in 13 adult *Tyr::CreER; BRaf*^{CA}*; Pik3ca*$^{lat/lat}$ mice and 8 weeks later they were randomized by tumor size and sex for treatment with GDC-0973 (2mg/kg, q.d., n=7) or GDC-0973 plus BYL719 (50mg/kg, b.i.d., n=6). Melanoma growth or regression was measured weekly over the course of 106 days of drug treatment. Tumor sizes were measured weekly and plotted as described previously, with error bars indicating SEM.

(E) A spider plot of the individual tumor response for each of the 13 mice treated in **(D)**. Horizontal dotted line indicates progressive disease when tumor volume was ≥100% of tumor volume prior drug treatment. Tumor sizes are displayed as the average percent change in tumor size from the start of treatment.